Dynamics of soil water potential as a function of stand types in a temperate forest: Emphasis on flash droughts

Blandine Courcot[1,2], Daniel Lemire[1], Nicolas Bélanger[1,2]

[1] Data Science Research Laboratory, Université du Québec (TELUQ), Montreal, Quebec, Canada; [2] Centre d'étude de la forêt, Université du Québec à Montréal, Montreal, Quebec, Canada

Highlights

- Hardwoods with a presence of beech have developed faster soil water potential regulation strategies.
- Beech trees act to conserve soil water by maintaining cooler soils and limiting water loss through evapotranspiration during flash droughts.

Abstract

In the context of a changing climate and the increasing occurrences of extreme events, including droughts, field evidence, and models suggest that cases of forest decline and migration of tree species to more suitable climates will augment in the 21st century. In northeastern North America, an expansion of American beech at the expense of maples has been observed since the 1970s and has been associated to several causes. Through an analysis of time series leveraging thousands of data collected in a temperate forest in southern Quebec, Canada, dynamics of soil water potential were analyzed in interaction with soil temperature, meteorological variables and forest types, including hardwoods (mostly maple) with a large presence of beech trees (hardwood-beech stands), hardwoods (maple and birch) and mixedwoods (maple and fir). During flash drought events with a net precipitation deficit and water stress, the presence of beech led to a decrease in soil temperature and favored the maintenance of low soil water potential and faster restoration of water reserves compared to mixedwoods. Using machine learning-based approaches, distinct critical soil temperature thresholds in regard to water potential were identified for the various forest types, and the temporality in soil water regime changes was more favorable under hardwood-beech stands. The presence of beech appears to render greater resilience in regard to water stress in this forest. A greater capacity of beech to preserve and restore soil water not only offers an additional explanation for its establishment in hardwoods in the last decades, but greater water conservation in the presence of beech, assuming it remains in the landscape, could also help local plant species adapt to climate change and to the predicted increased water deficits, as well as species migrating northward to find more suitable environmental envelopes.

Keywords

soil water potential, flash drought, dry-down, forest species composition, ecological memory, changing states.

Introduction

Global warming is expected to be coupled with increased drought events and a shift towards a new baseline of megadroughts and pluvial conditions (Stevenson et al., 2022). In many regions, it is predicted that droughts will establish more rapidly, be more frequent and severe and last longer (Trenberth et al., 2014; Samaniego et al., 2018). Warmer air temperatures and in turn increased evaporative demand will lead to very large soil water deficits in already sensitive semi-arid regions (e.g., Bonsal et al., 2013; Williams et al., 2020). For areas with intrinsically higher moisture such as temperate regions, models to predict water stress over the next decades are associated with greater uncertainties (Houle et al., 2012; Cholet et al., 2022), but global predictions nevertheless lead toward

a loss of soil water availability. In northeastern North America, for example, Houle et al. (2012) predicted that forest soil water availability could be decreased by as much as 40% towards the end of the 21st century. Similarly, Cholet et al. (2022) modeled soil water potential in forests of eastern North America using the Canadian Land Surface Scheme (CLASS) under RCP8.5 and predicted that in Wal water stress will increase in severity by 33 % and in duration by 158% compared to current levels. They also found that soil depth and texture were the main variables controlling water stress and that large increases in duration are expected in areas with already prolonged droughts.

Excess forest mortality is now being observed all over the world and is often linked to the increase in drought episodes, especially in more arid environments (Breshears et al., 2005; Allen et al., 2010; 2015; Greenwood et al., 2017; Hammond et al., 2022). Following a series of droughts in the 1980s and thereafter, massive episodes of dieback of trembling aspen forests in the semi-arid Prairie provinces are the most compelling evidence of tree mortality due to water stress in Canada (Hogg et al., 2002; Michaelian et al., 2011). Some of these dieback episodes were closely linked and exacerbated by defoliators. For the Canadian boreal forest, Peng et al. (2011) reported that tree mortality increased by an average of 4.7 % per year between 1963 and 2008, with a higher rate in the west compared to the east. Regional droughts were suggested as the main factor controlling the mortality increase. In the boreal forest, the impact of sequential years under low-intensity dry conditions appears to be a better predictor of tree mortality than the intensity of the most severe droughts (Sánchez-Pinillos et al., 2022). Temperate forests are also negatively affected by water stress, although recent studies more often report growth declines due to drought than mortality, but the mortality risk is associated with low resilience to drought (Brzostek et al. 2014; D'Orangeville et al. 2018; Senf et al. 2020; Hammond et al. 2022; Lloret et al. 2022; Martinez del Castillo et al., 2022; DeSoto et al., 2020).

Conversely, repeated exposure to droughts promotes ecological memory that can make trees more resilient to water stress (Ogle et al., 2015; Yao et al., 2022). The ecological memory of an ecosystem regarding past climatic events can largely shape its resilience to upcoming climatic events (Johnstone et al., 2016). Drought legacy is modulated by tree species and ecosystems and could impact tree growth and survival (Anderegg et al., 2015 ; Kannenberg et al., 2020). Moreover, transient droughts could have a lesser impact on trees with a longer memory when their growth depends on longer periods of precipitation (Peltier et al., 2022). Pre-drought stand characteristics, including forest structure, diversity and past management, are also important to take into consideration when predicting the impacts of water stress on tree growth and mortality (Lloret et al., 2022). In this respect, some adaptative management schemes could be implemented (e.g., thinning and selecting drought-tolerant species) to better manage water and protect forest landscapes in the context of climate change (Grant et al., 2013). Yet, the challenge of adapting forests to climate change, and thus increased droughts, also lies in the identification of forest parameters that buffer the effects of the expected increase in evaporative demand. Although many studies have focused on the sensitivity of forests and trees to drought events, there are very few studies looking at key parameters that render the ability of a forest to preserve soil water *per se* under increasing evaporative demand. Some soil moisture indices such as the Standardized Precipitation Evapotranspiration Index (SPEI) yield fine-scale variations in soil moisture and can be useful for water management and decision-support purposes (Begueria et al., 2014). However, these indices are criticized because their parameterization is based on climate data alone, so they mainly calculate the difference between precipitation and evapotranspiration (Berg and Sheffield, 2018; Cholet et al., 2022). These indices likely overestimate evaporative demand because they fail to account for the buffering effect that some key ecosystem characteristics can exert, including soil features (i.e., texture, organic matter content and depth) as well as forest features (i.e., structure, composition and litters). Are there forest types that more efficiently preserve soil water reserves during droughts? If so, do these forest types delay the transition from one soil water state, considered as normal, to a new one, such as a soil water deficit for plant growth and survival? A tree species or forest type that can withstand a change of state in available water will likely be more ecologically resilient to climate change (Holling, 1996; Hesse et al., 2023).

In this respect, soil water potential was monitored for four years at high spatial and temporal resolutions at a forest site in southern Quebec, Canada, where forest species composition varies from

mixed stands (hardwoods and conifers) to maple-birch and maple-beech stands. Periods of water stress were captured, including flash droughts induced by an absence of precipitation (some during heatwaves) and during which a dry-down was recorded based on a constant decrease in soil water potential (McColl et al., 2017) followed by a rapid recovery rate (Pendergrass et al., 2020). By combining modeling and statistics, a large time series database of soil water potential was analyzed to test the two following research questions: (1) Can the different states in soil water potential be defined and can the frequencies and probabilities associated with the changes in states over time and across the three forest types be determined? (2) Focusing on extreme climatic events such as flash droughts, do forest types respond differently to water stress?

Materials and Methods

Study location and experimental design

The study was conducted at the *Station de Biologie des Laurentides* of *Université de Montréal*, located in St. Hippolyte (Quebec, Canada), 80 km north of Montreal (45°59'N;74°0'W). The site is located at the northern limit of the sugar maple and yellow birch (*Betula alleghaniensis*) bioclimatic domain (Saucier et al., 2009). The dominant tree species at the site include sugar maple, American beech, yellow birch, red maple (*Acer rubrum*), white birch (*Betula papyrifera*), largetooth aspen (*Populus grandidentata*), eastern white cedar (*Thuja occidentalis*), red spruce (*Picea rubens*) and white pine (*Pinus strobus*), as well as species commonly found in the boreal forest such as balsam fir (*Abies balsamea*) and white spruce (*Picea glauca*). According to output from the BioSIM model (Régnière and Saint-Amand, 2017), the average annual temperature at the site between 2003 and 2013 was 4.9 °C, and the average precipitation over the same period was 1270 mm, including 30% falling as snow. Soils are classified as Orthic Humo-Ferric and Ferro-Humic Podzols with a sandy loam texture and the forest floor is characterized by a moder humus form (Soil Classification Working Group, 1998; Bélanger et al., 2012, 2021).

The experimental design covers an area of 18 hectares, with height blocks of four plots (3 × 3 m) distributed in three areas, for a total of thirty-two plots. Each block, with a minimum area of 0.5 hectares, is characterized by a homogeneous forest stand type (Bélanger et al., 2021). The blocks include three main forest types: (1) mixedwoods (MW), composed mainly of balsam fir and deciduous trees, (2) hardwoods (HW), composed mainly of sugar maple, red maple and birch spp., and (3) hardwood-beech (HB) stands, composed mainly of sugar maple and American beech. Block classification was based on various criteria. For instance, a station was classified as mixedwoods when its total basal area was at least 20 % of balsam fir (blocks 1, 4 and 7). To differentiate between hardwoods and hardwood-beech stands, litter composition was used, i.e., when 20 % of the total litter mass originated from beech, the block was classified as hardwood-beech stands (blocks 3, 5, and 8), whereas hardwoods presented less than 20 % (blocks 2 and 6). Full details of the experimental design and classification criteria are provided in Bélanger et al. (2021). Each plot was equipped in spring 2017 with two probes (A and B) measuring soil temperature (Spectrum Technologies, United States) and two probes (C and D) measuring soil water potential (200SS Watermark, Irrometer). They were positioned at a depth of 10-12 cm and connected to the same data logger (WatchDog 1650 Micro Station, Spectrum Technologies). This depth corresponds to the transition between the forest floor and mineral soil, where 80% of the root biomass is found, as well as to the depth of heating cables which were also installed during spring 2017 but only turned on in November 2020. Therefore, the probes monitor the effect of heating cables, but in this study, data were analyzed before the cables were turned on. Data were monitored every 15 minutes. Soil water potential with these probes ranges from 0 to 200 kPa, characterizing soil as either very wet or very dry, respectively (the negative sign is omitted considering implicitly the potential as a tension). Data from loggers were retrieved several times between May and October and then formatted for Matlab R2022a, which was used for subsequent analyses. For the four years of interest, from May 2017 to October 2020, a total of 1,696,473 observations (i.e., soil temperature and water potential) were measured and collected.

Several probe models offer more range and precision than the 200SS Watermark probes (Payero et al. 2017), but the former probes have a much greater cost than the latter. Furthermore, the 200SS Watermark probe is designed to be permanently installed and is not harmed by freezing which is a concern in soils at the study site. It is composed of two corrosion-resistant electrodes that require a minimal power requirement (2.5V), a ceramic disk, and a granular matrix in a stainless-steel enclosure. As water enters the granular matrix, the probe measures the change in electrical resistance which is proportional to the change in soil water potential. These data are converted into kPa based on a calibrated equation (Shock et al. 1998). Furthermore, significant variability in soil water potential can arise naturally because of heterogenous soils, and it can also come from technical problems with measurement devices and human or logistical errors (e.g., poor probe installation), which can all lead to different responses between two identical probes located nearby in the same plot. Our analytical strategy thus relied on two experimental specificities: (1) the deployment of a large number of probes to capture spatial variability as much as possible and to increase the scale of analysis from the plots to the stands (which means a possible combination of two or three blocks of four plots), and (2) a very high sampling frequency corresponding to a 15-minute period. The compromise of deploying a large and permanent network of 200SS Watermark probes to capture spatial variability in soil water potential at the cost of some precision and range is also reasonable considering that the depletion in available soil water holding capacity of a sandy soil, such as the one at the study site, is reflected by lower soil water potential than a heavier soil. For example, Irmak et al. (2016) suggested ranges of irrigation trigger points between 30 and 33 kPa for a sandy loam soil and between 75 and 80 kPa for a silty clay loam soil.

Climatic data between 2017 and 2019 were modeled with BioSIM, and starting in 2020, a complete meteorological station (Campbell Scientific) was installed at the study site. Using site elevation, latitude and longitude, BioSIM uses multivariate regressions to extrapolate data from the closest weather stations specifically in eastern North America (Régnière and Bolstad, 1994). The daily meteorological variables generated using BioSIM were considered exogenous variables, i.e., independent variables for which measurements are not conducted within the soil water potential model that is developed. They included air temperature (Tair) in °C, precipitation (Prcp) in mm, relative humidity (RelH) in %, and solar irradiance (SRad) in W m^{-2}. Vapor pressure deficit (VPD) expressed in kPa was used as an integrative variable. It was calculated using the Tetens' equation (Tetens, 1930), which was reformulated by Monteith and Unsworth (2007) for air temperatures above 0 °C. The only independent variable for the model that was measured within the soil is temperature (Tsoil), expressed in °C, which was collected from the probes in the plots, as indicated above.

Data cleaning and the data processing pipeline consisted of eight main steps that allowed time series analysis and forecasting: (1) outlier removal, which aimed at removing aberrant data from soil temperature probes. The criteria for removal were temperatures below -20 °C and above 46 °C during the periods of interest (May to November for each year); (2) adjustment of soil water potential based on soil temperature measurements according to the equation in Irmak et al. (2016); (3) data sampling to reduce signal-to-noise ratio and variability for temperature (probes A and B) and soil water potential (probes C and D). Two default sampling frequencies were used, i.e., averaging across one hour and across one day. Sampling was conducted for each plot, each block and each forest type, resulting in average soil water potential and temperature for each case, along with calculated uncertainties; (4) data regularization using cubic BSpline interpolation to obtain measurements at each time point and to regularize time series with no missing data points; (5) data smoothing using a Savitzky-Golay filter (6th-degree polynomial) with a 3-day centered moving average. Smoothing was performed after data averaging to reduce noise by a factor equal to the square root of the number of measurements (Savitzky and Golay, 1964). This selected low-pass filter ensured that extreme values in the database were not sacrificed; (6) meteorological data processing and synchronization, based on a one-hour and one-day sampling of meteorological data from BioSIM, as well as regularization of time series for data synchronization with soil water potential and temperature data; (7) temporal interval selection for each studied year based on the plot with the smallest observation interval. Time intervals, aligned with snow-free period on the soil, were standardized for each year as follows: May 11 to October 29 for

2017, May 24 to November 7 for 2018, May 8 to November 10 for 2019, and May 1 to October 23 for 2020; and (8) analysis of flash droughts, which consisted of identifying flash drought periods (8 days or more without precipitation) where soil water potential increased to near-maximum values (i.e., 200 kPa). The choice of an 8-day threshold for flash drought periods aligns with the study by Fu et al. (2022), considering that consecutive days without precipitation lead to soil moisture declines. In the biogeographic and climatic contexts of this study, this shorter period included more drying periods for analysis.

Time series analysis

A categorical variable representing the states of soil moisture (StateSM) was introduced to describe soil water potential. Three main tension levels were defined, i.e., low, medium and high. Soil water potential thresholds (kPa) were set for each level. To do so, soil water potential density curves were first calculated for each stand and the four monitoring years, which allowed to identify preliminary thresholds. In the absence of irrigation thresholds in the scientific literature for forestry that are based on measurements made with 200SS Watermark probes, irrigation thresholds reported for crops using similar resistance soil water potential measurement techniques were also used to validate threshold selection (Shock and Wang, 2011). Some useful scenarios were for sandy soils and included potato (irrigation trigger points between 20 and 60 kPa), cauliflower (trigger points between 20 and 40 kPa) and celery (trigger point around 10 kPa). The three following thresholds were established as follows: (1) *low* state, corresponding to a soil water potential in the range [0 kPa, 40 kPa[(2) *medium* state, corresponding to a soil water in the range [40 kPa, 100 kPa[and (3) *high* state, corresponding to a soil water potential equal or greater than 100 kPa. For some analyses, a fourth state was considered, i.e., *very high* state. In this case, the *high* state corresponded to a soil water potential between in the range [80 kPa, 120 kPa[and the *very high* state corresponded to a soil water potential equal or greater than 120 kPa. Increasing the number of levels allows for a better description of high potential values, but it also decreases the predictive capacity of models because *high* and *very high* states have fewer observations than the *low* and *medium* states, thus leading to imbalanced conditions.

Because soil water potential is described by its value at each time point and by its states, the evolution of these states was depicted by determining the transition probabilities from one state to another and the expected number of days to reach them. To do this, time series were expressed using discrete-time Markov chains. Discrete-time Markov chains are used to elucidate dynamic systems governed by stochastic processes. By exploiting the temporality of soil water potential data and relying on the postulate of the Markov property, transitions that occurred during each year of interest could be analyzed in detail. This analysis involved calculating the probabilities associated with each observed state change and evaluating the expected time to attain these states.

Cross-correlations at *lag-k* between two discrete time series x(n) and y(n) were calculated to evaluate their similarity considering the following:

$$R_{xy}(k) = \sum_{n=k}^{N-1} x(n).y(n-k) \quad (1)$$

where x(n) represents the value of x at time index n, y(n-k) the value of y at time index (n-k), i.e., with a k-lag, and N is the number of time steps considered. The xcorr() function implemented in Matlab was used.

To refine the analysis of the evolution of soil water potential states, classification methods based on supervised learning such as decision trees were considered. Classification and Regression Tree (CART) algorithm was used (Breiman et al., 1984).

Finally, when focusing on flash drought periods, data 8 days before and 8 days after the dry-down were extracted for a better understanding of how soil temperature and soil water potential evolve concomitantly.

Results

Large variations in soil water potential were observed based on year and forest types (Figure 1). In particular, in 2020 and for the three forest types, soil water potential reached very high values (i.e., low soil water availability) in the late spring to early summer period (mostly in June), which distinguished them from the three other years of interest. Precipitation amounts in June 2020 were particularly low, especially in May and June, which impacted soil water potential during that period (Figure S1, supplementary data). Conversely, the year 2017 exhibited the lowest soil water potential values, which likely reflects a period needed for the probes to stabilize in the soil after their installation in spring 2017, although it was also one of the wettest years. Based on forest types, peaks in soil water potential between 2018 and 2020 were classified in the following increasing order: hardwood-beech stands < hardwoods < mixedwoods (Figure 1).
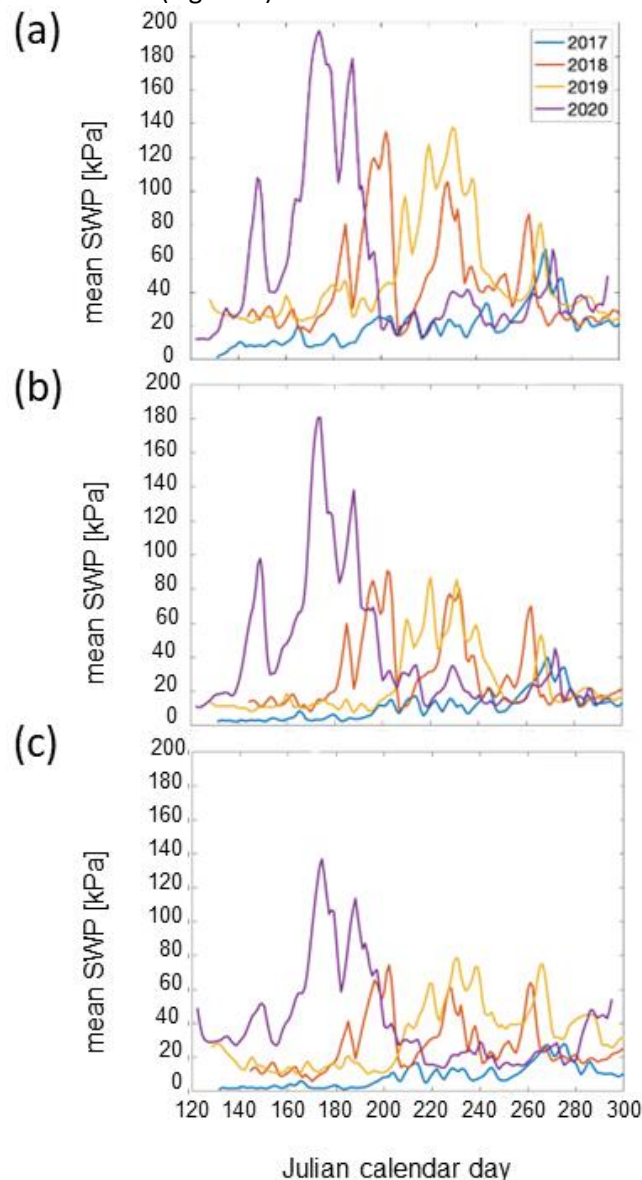

Figure 1: Mean daily soil water potential (SWP) in kPa for (a) mixedwoods, (b) hardwoods and (c) hardwood-beech stands from 2017 to 2020.

As discussed in the methods, three main soil water potential states [0; 40[kPa (*low*), [40; 100[kPa (*medium*) and [100; 200] kPa (*high*) were defined by setting arbitrary thresholds comparable to studies using the same soil water potential probes. Using discrete-time Markov chains, it was possible

6

to isolate differences in state transitions within the same stand and for a specific year. For mixedwoods in 2019, it took 81 days to reach a high state of soil water potential from a medium state (Figure 2). In 2020, the expected time for this transition in soil water potential states to occur was established at 63.5 days, and this transition was more likely in 2020 than in 2019, with a transition state probability of 0.06 compared to 0.04.

This approach also emphasizes differences in response between mixedwoods and hardwood-beech stands in the *medium* to *high* and *high* to *medium* transitions. In 2020, mixedwoods required much fewer days (63.5 days)) compared to hardwood-beech stands (117 days) to transition from a soil water potential considered as a *medium* state to a soil water potential considered as a *high* potential state (Figure 3). Furthermore, for the same year, mixedwoods remained in a *high* soil water potential state longer (14 days) compared to hardwood-beech stands (6 days) (Figure 3).
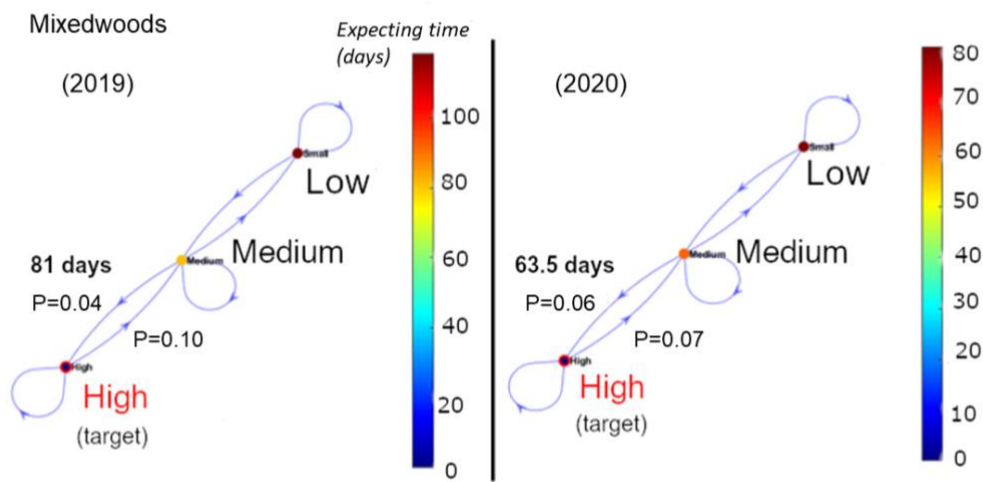

Figure 2: Transition state probabilities (denoted as P) and expected time in days to reach a *high* state of soil water potential starting from a *medium* state for mixedwoods stands in 2019 (left panel) and 2020 (right panel). The color scale indicates the number of days and the target states are indicated in red. The soil water potential states are as follows: [0; 40[kPa is *low*, [40; 100[kPa is *medium*) and [100; 200] kPa is *high*.
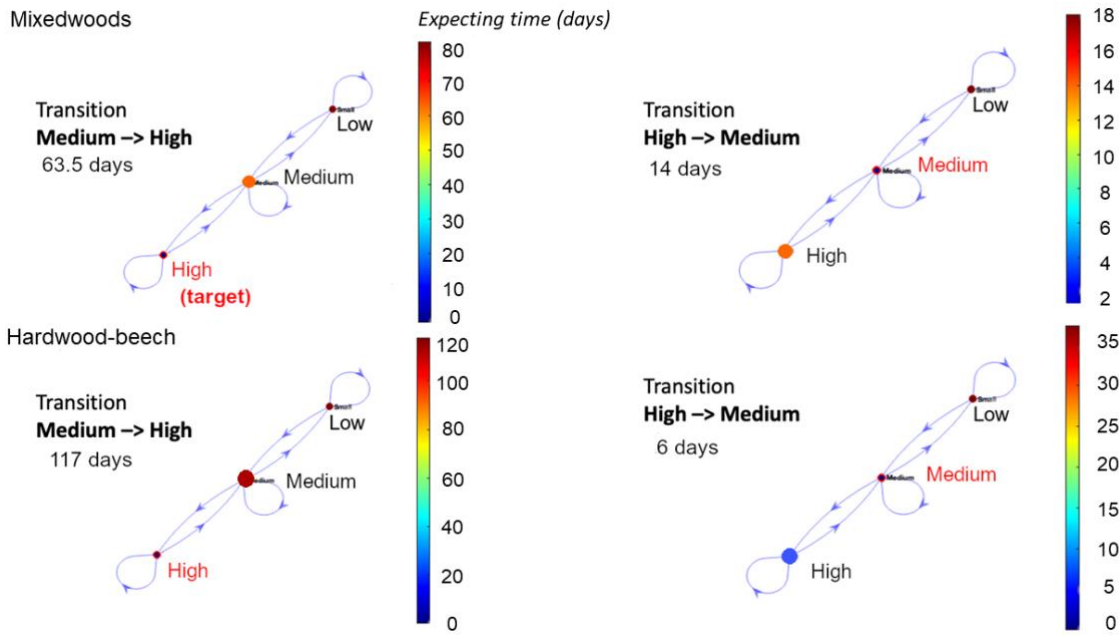
Figure 3: Expected times in days to reach *medium* (right panels) and *high* (left panels) states of soil water potential for mixedwoods (upper panels) and hardwood-beech stands (bottom panels) in 2020. The color scale indicates the number of days and the target states are indicated in red.

Cross-correlation analysis reveals that each forest type exhibits different correlations with soil water potential over time (see Figure 4 for qualitative results and Tables S3, S4 and S5 for coefficients). Although the maxima represented by darker colors often occur at similar time lags for most variables (except for relative humidity), the correlations weaken at different time steps expressed in days. This is the case for vapor pressure deficit which influences soil water potential in mixedwoods for up to six days after the highest soil water potential value is reached (see Figure S2 for dynamics of vapor pressure deficit in 2020).

For hardwoods and hardwood-beech stands, the same effect of vapor pressure deficit is sustained for up to five and four days, respectively. The influence of soil temperature over soil water potential is maintained for up to three (hardwood-beech stands) and two (mixedwoods and hardwoods) days (Figure 6). At (t-4 days), the coefficient only slightly decreases compared to the coefficient at day (t). The influence of relative humidity reaches a maximum two days before the soil water potential maximum value in hardwood-beech stands, whereas this effect is the largest five and six days before maximum values in mixedwoods and hardwoods, respectively (Figure 4). Mixedwoods and hardwoods show very comparable cross-correlations, whereas cross-correlations for hardwood-beech stands between some exogenous variables and soil water potential seem to stand out, notably with relative humidity and vapor pressure deficit (Figure 4).

For all three forest types, soil water potential and air temperature show a maximum cross-correlation without any lag, which means that no previous or subsequent influence of air temperature on soil water potential has been detected.
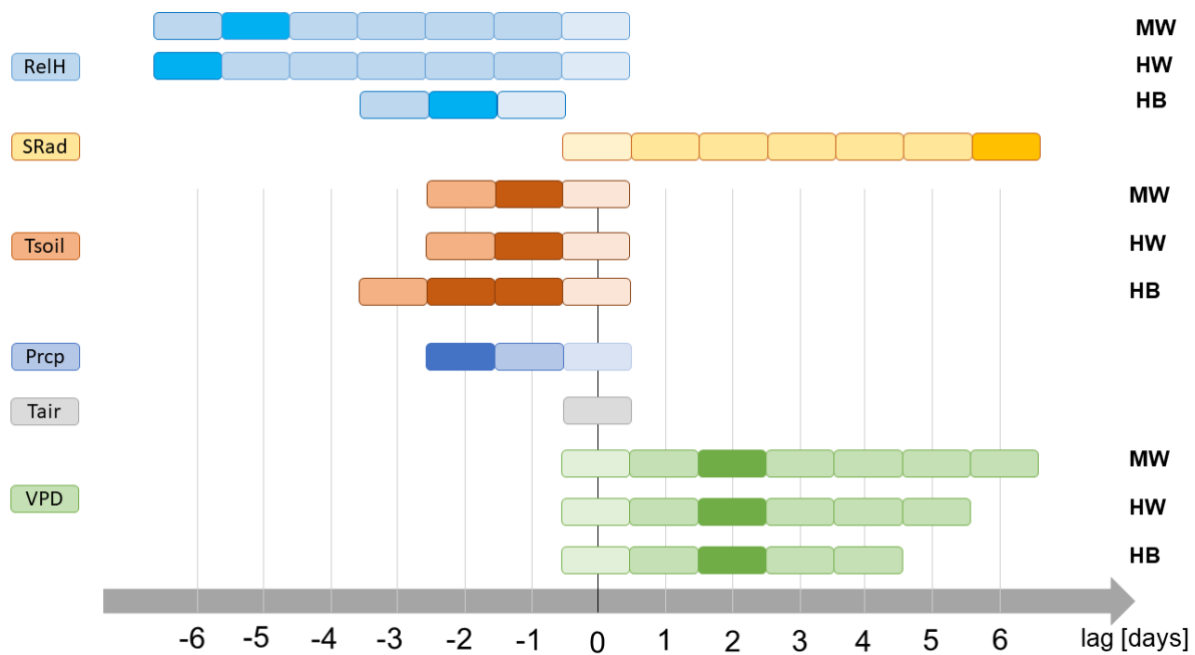
Figure 4: Diagram summarizing cross-correlations coefficients between soil water potential and exogenous variables and soil temperature (2020). Tsoil is soil temperature, Tair is air temperature, Prcp is precipitation, RelH is relative humidity, VPD is vapor pressure deficit, SRad is solar radiation. Calculations were performed on the 2020 data for each forest type (MW is mixedwoods, HW is hardwoods and HB is hardwood-beech stands). The maximum cross-correlation coefficient is represented by a darker color rectangle. For Tair, SRad and Prcp, the same results are obtained for the three stands, thus only one series of rectangles are shown. Coefficient values are available as supplementary data.

The dynamics of soil water potential were investigated concomitantly with precipitations and soil temperature during flash drought periods for each forest type in May, June and September 2020 (Figure 5, 6 and 7, respectively). The flash droughts in May and June behaved similarly, i.e., soil water potential increased throughout the periods, whereas the daily average soil temperature of hardwood-beech stands remained lower than that in mixedwoods and hardwoods. For mixedwoods, soil water potential reached values above 100 kPa in May (Figure 7a) and close to 200 kPa in June (Figure 8a). Soil water potential values in hardwoods were slightly below those in mixedwoods. For hardwood-beech stands, soil water potential also increased but maximum values were lower than the two other forest types at 40 kPa in May and 140 kPa in June.

On May 26, 2020, there was trace precipitation (< 1 mm) which did not decrease soil water potential (Figure 5a). Soil water potential decreased only on May 28 and 29 when precipitations were more abundant (~3 and 8 mm, respectively). Before, during and after the first two droughts in May and June, soil temperature in hardwoods was higher than in the two other forest types (Figure 5b, 6b). In May 2020, soil temperature in mixedwoods was slightly above that in hardwood-beech stands only during some days. However, in June 2020, a larger and more sustained divergence in soil temperature between mixedwoods and hardwood-beech stands was observed, with mixedwoods having warmer soils. The colder soil in hardwood-beech stands was especially apparent during the dry-down between June 12 and 22 (Figure 6b).
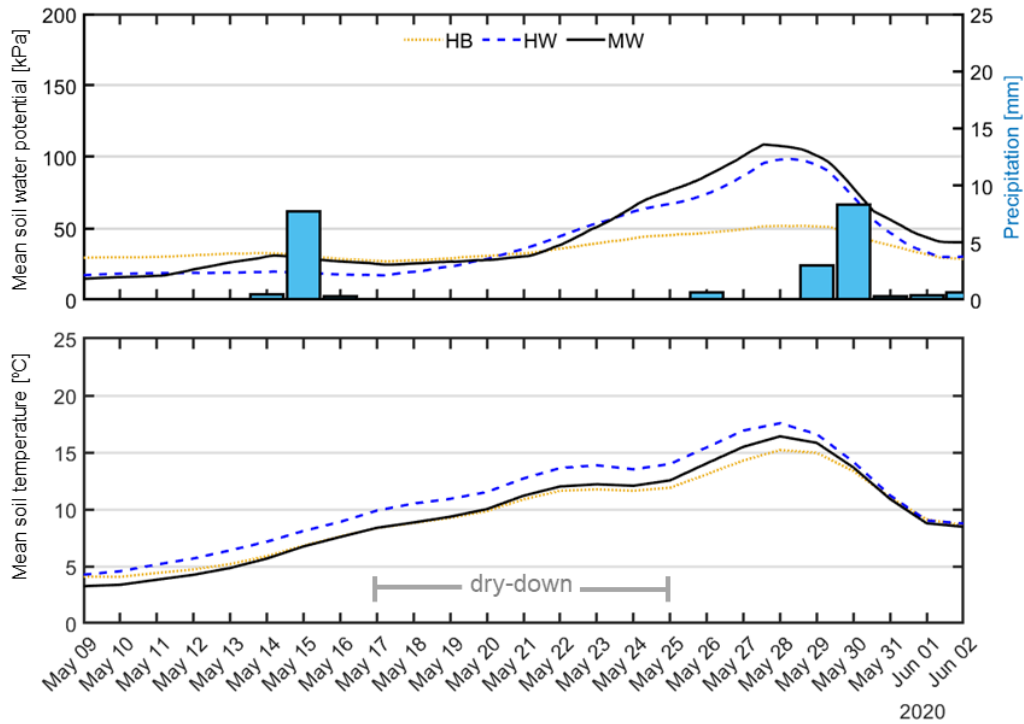
Figure 5: Mean daily soil water potential along with precipitation in mm (upper panel) and soil temperature in °C (lower panel) for mixedwoods (MW), hardwoods (HW) and hardwood-beech stands (HB) during the first flash drought in May 2020 (same scales as Figures 8 and 9 for comparison).

In September 2020, differences in soil temperature between forest types were less apparent compared to May and June (Figure 7b). On September 18, i.e., at the onset of the dry-down, soil water potential was 32 kPa in mixedwoods compared to about 20 kPa in hardwoods and hardwood-beech stands (Figure 7a). At that time, soil water potential in mixedwoods exhibited a more pronounced dry-down than that in hardwoods and hardwood-beech stands, thus reaching a *medium* state faster. At the end of the dry-down, soil temperature of hardwood-beech stands was also lower than that of mixedwoods and hardwoods, but to a lower extent compared to the previous flash droughts in May and June. The pattern of a lower soil temperature in hardwood-beech stands at the end of a dry-down compared to mixedwoods and hardwoods was also observed in 2018 and 2019 (Figure S3, supplementary data).
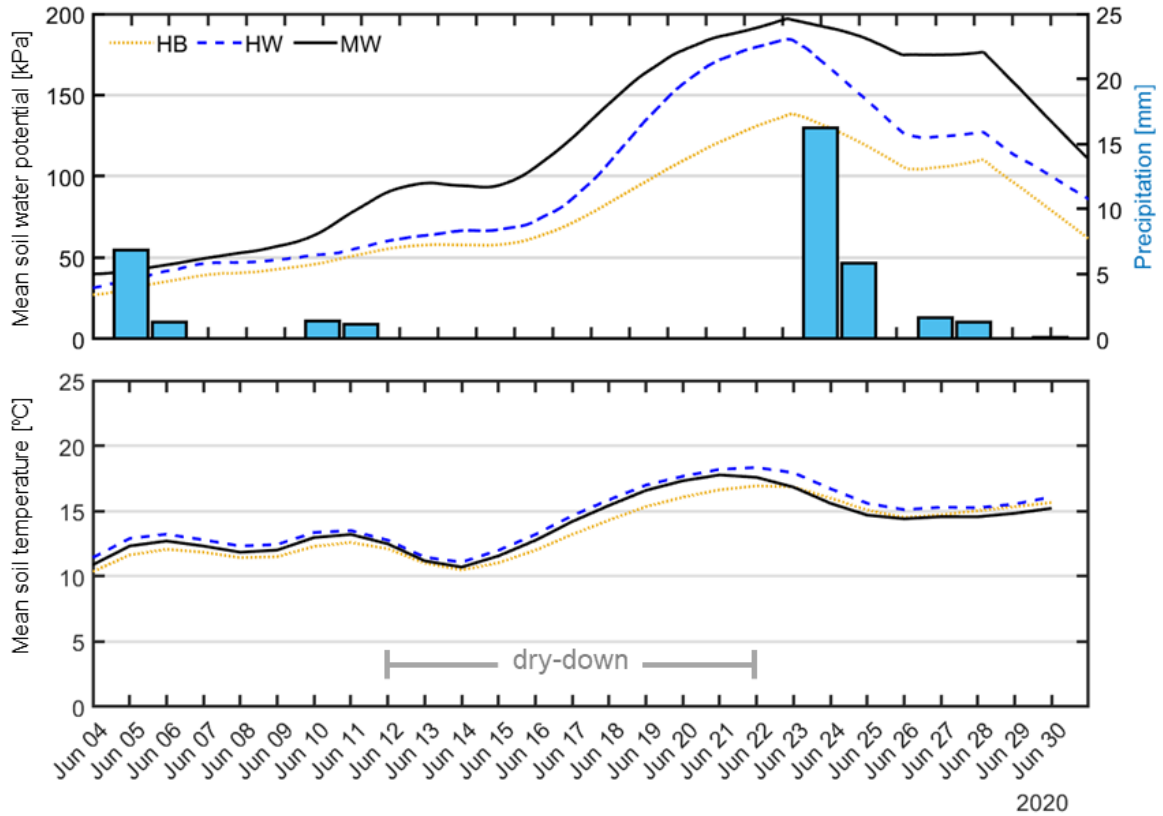
Figure 6: Mean daily soil water potential along with precipitation in mm (upper panel) and soil temperature in °C (lower panel) for mixedwoods (MW), hardwoods (HW) and hardwood-beech stands (HB) during the second flash drought in June 2020 (same scales as Figures 7 and 9 for comparison).

The distinct behavior of hardwood-beech stands regarding soil water potential and temperature during flash droughts is also described using decision trees and considering the three main soil water potential states (*low*, *medium*, *high*) as well as a fourth state (*very high*, > 120 kPa). Figure 8 compares the decision tree trained with data from mixedwoods to the decision tree trained with data from hardwood-beech stands during the most severe flash drought registered during the year of interest, i.e., June 2020. For mixedwoods, the transition to a *very high* state of soil water potential occurs for a soil temperature greater than or equal to 12.9 ◦C. For hardwood-beech stands, soil water potential reaches this same state for a soil temperature greater than or equal to 15.9 ◦C.
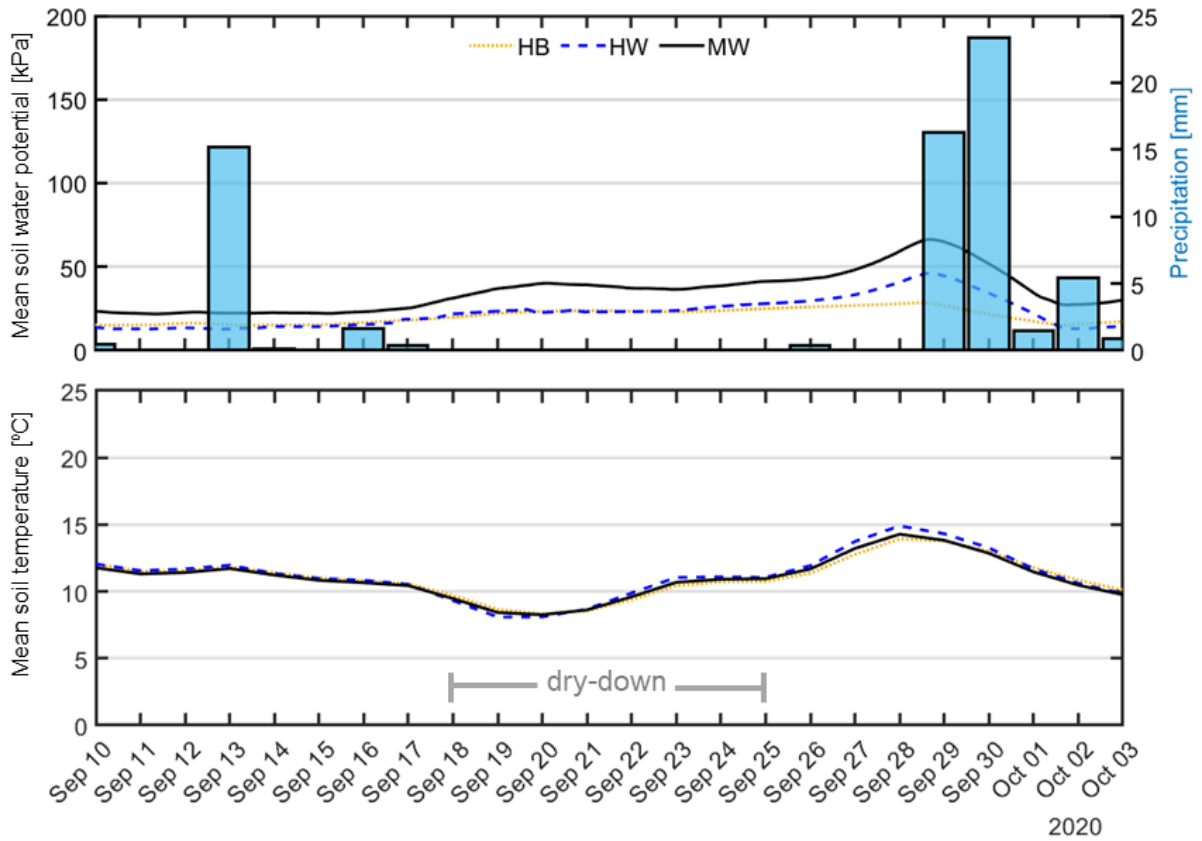
Figure 7: Mean daily soil water potential along with precipitation in mm (upper panel) and soil temperature in °C (lower panel) for mixedwoods (MW), hardwoods (HW) and hardwood-beech stands (HB) during the third flash drought in September 2020 (same scales as Figures 7 and 8 for comparison).
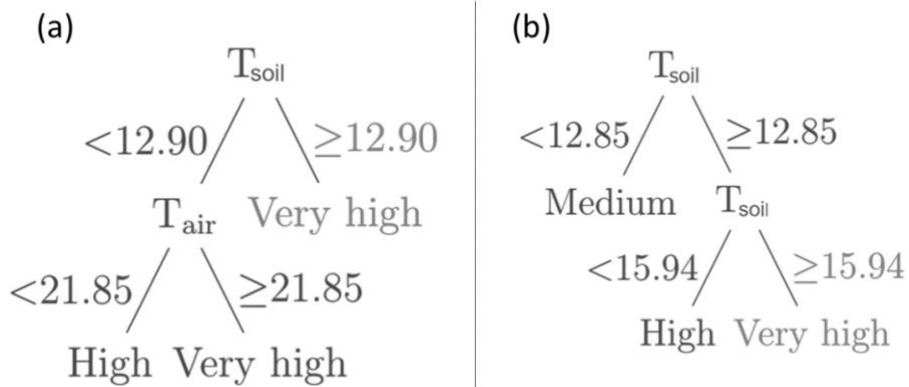

Figure 8: Decision tree obtained for (a) mixedwoods and (b) hardwood-beech stands during the second flash drought of June 2020, i.e., the most severe recorded during the four years of record. The soil water potential states are as follows: [40; 100[kPa is *medium*, [80; 120[kPa is *high* and [120; 200] is *very high*. Temperatures are in ◦C.

Discussion

Changes in soil water states and lagged effects

Using a discrete-time Markov chain approach, it was possible to calculate frequencies and probabilities associated with transitions between soil water potential states, addressing the first research question. Results from this analysis suggest a higher resistance of hardwood-beech stands to changes in soil water potential states compared to hardwoods and mixedwoods. Such resistance to change is often indicative of greater ecological resilience (Holling, 1996; Hesse et al. 2022). The use of Markov chains appears relevant for describing the dynamics of soil water potential and results indicate a trend toward greater resilience of hardwood-beech stands to water stress. The next challenge is to define the transition thresholds with more detail. This could be done experimentally using more accurate sensors and simulating various level of drought stress (Walthert et al., 2021). One of the limitations of this analysis lies in the Markov property, which assumes that the prediction of the future is entirely contained in the present state of the process. Therefore, the correlations between variables over time help to fully describe the physical phenomena.

Cross-correlations results also show the specificity of each forest type and bring attention to the concept of memory or lagged effect as designated by Zhao et al. (2018). Drought memory (or drought legacies) alters tree physiological processes such as growth and its effects are largely demonstrated as a function of species and different spatial (e.g., communities and ecosystems) and temporal scales (Müller and Bach, 2022). Plant resilience depends on the memory of an ecosystem which is shaped by past events, and as the frequency of droughts increases, ecosystems can build ecological resilience (Johnstone et al., 2016; Yao et al., 2022). On the other hand, the legacy of hydraulic failure could reduce resilience, especially regarding tree's xylem experiencing embolism (Hammond, 2020). Hence, incorporating the concept of lagged effects into models can improve predictions of tree recovery or death following droughts (Peltier et al., 2022). Several physiological mechanisms come into play at cellular levels (Daszkowska-Golec and Szarejko, 2013). For example, phytohormones control the closure of stomata in isohydric species (which decreases photosynthetic and transpiration rates) to maintain a lower water tension (i.e., a higher water level) during water stress under high vapor pressure deficit (McDowell et al., 2008; Grossiord et al., 2020a; Chen et al., 2022). In contrast, anisohydric species keep their stomata open to continue drawing water from the soil, thus allowing their water tension to rise (McDowell et al., 2008). In the short term, stomatal closure is the main mechanism for plants to limit transpiration losses and to control water tension levels (Martinez-Vilalta et al., 2014), and adjustments to higher air temperatures can occur within a few hours (Grossiord et al., 2020a). The concept of isohydric and anisohydric species to group plant species as either vulnerable or well adapted to climate change and increased droughts is under debate, however (Martínez-Vilalta et al., 2017; Ratzmann et al., 2019). Notably, beech trees are mostly considered to behave as anisohydric species (Rukh et al., 2023). Nevertheless, in this study, results suggest a closer behavior to isohydric species with less drought sensitivity (Pretzsch et al., 2020; Motte et al., 2023). This relates to the idea that trees can switch between iso- and anisohydric behavior due to environmental conditions and growth developmental stages (Meinzer et al., 2016).

The concept of soil moisture memory has also been studied but to a much lesser extent. Soil moisture is controlled by evapotranspiration and evaporative demand (Koster et Suarez, 2001; Seneviratne et al., 2010), but also by the storage capacity of the soil (Walthert et al., 2021) and the stomatal control of the trees, as well as soil microbial communities that use and affect the availability of carbon and nitrogen (Jacques et al., 2021). Periodic droughts contribute to the ecological memory of soils by increasing their multifunctionality (expressed as enzymatic and microbial activities, nutrients, root growth), making them more resilient to water stress (Canarini et al., 2021). Orth and Seneviratne (2012) determined that the effect of soil moisture memory could last up to 40 days and depends on the season, with larger effects during dry periods on the wettest sites. The existence of a positive stress zone as introduced by Kögler and Söffker (2020) hence aligns with both trees and soils. However, monitoring of soil water potential in this study is limited in the sense that, although most root biomass is in the first 25 cm of soil at the study site (Lajeunesse, 1990), many trees will have

developed deep roots that can fulfill water requirements, notably during droughts (Nelson and Oliver, 2017; Chen et al., 2022). Thus, placing some probes at greater depths (e.g. 50 cm) would have given a fuller portrayal of soil water availability for trees at the site.

Yet, there is limited literature on how various forest types can preserve soil water during drought periods. Results in this study from discrete-time Markov chains and decision trees suggest that soil water potential in mixedwoods is more easily and rapidly shifted toward high values during dry periods and that hardwood-beech stands resist this shift for longer during droughts, with a faster return to lower water potential as well. During droughts in 2020, classification and regression trees suggest that the transitioyn to very high soil water potential, i.e., exceeding 140 kPa, occurred for hardwood-beech stands at a soil temperature of 15.9 °C compared to a transition at 12.9 °C in mixedwoods. It is suggested that this 3 °C divergence could be quite meaningful in regard to forest management and adaptation to climate change. According to Forzieri et al. (2022), 23% of the world's pristine forests have already reached a critical threshold that leads to decline and loss of resilience, likely because of water limitations and climate variability. Therefore, managing and adapting forests as a means to preserve soil moisture reserves under climate change is a priority (Grant et al., 2013).

The case of American beech

The persistence of American beech in the landscape is debated (Stephanson and Ribarik Coe, 2017). Although results in this study illustrate that it is perhaps more robust to climate variation and water limitations, the literature suggests that American beech is more sensitive to both droughts and flooding compared to other deciduous tree species. This idea is reinforced when considering European beech (*Fagus sylvatica*) (Geßler at al., 2007). However, Hesse et al. (2023) underlined that for a longer time scale (i.e., after 5 years of recurrent summer droughts), the recovery of Norway spruce (*Picea abies*, an isohydric species) is significantly slower than European beech (an anisohydric species) for many physiological variables tested, although both species recovered well. Therefore, beech trees seem more drought resilient than initially believed and this places doubt in regard to strictly categorizing beech spp. in the anisohydric group *per se*.

Two main reasons can be put forward to explain the strategy of hardwood-beech stands to more easily and rapidly shift toward a lower state of soil water potential compared to other forest types, especially mixedwoods. First, American beech is recognized for its dense canopy, which limits light from reaching the soil surface, and for its acidic and recalcitrant litter which creates a thick and protective leaf mat, all of which protect soils from direct radiation and lead to cooler soils with less evaporation and in turn, more moisture (Collin et al., 2017b; Bélanger et al. 2021). Second, like isohydric species, adult American beech trees could have a more effective stomatal regulation under drought stress (Leuschner, 2020), and similar to European beech trees, can save water during short period of stress, thus being more conservative in their water use strategies (Walthert et al., 2021 ; Puchi et al., 2024). A combination of both strategies is possible. However, during flash droughts, the capacity of hardwood-beech stands to preserve soil moisture diminished as the soil temperature increased. The buffering ability of hardwood-beech stands reached a limit when soil water was low as observed by the small difference in soil water potential between mixedwoods and hardwood-beech stands. This is an expected behavior because as the soil dries, water, with its specific latent heat, retains energy more effectively than the soil, which means that dry soil is more prone to overheating than moist soil (Fu et al., 2022). Finally, from a physiological standpoint, American beech distinguishes itself from other tree species by presenting adjustments characterized as a "fast ecological strategy" (Nikolova et al., 2020).

In temperate forests of northeastern North America, the expansion of American beech has occurred at the expense of other species, including sugar maple (Cale et al., 2017; Collin et al., 2017a; 2017b; Nolet and Kneeshaw, 2018; St Jean et al., 2021). Several hypotheses for this phenomenon were proposed, including roots sprout and effective regeneration, low leaf palatability, high tolerance to low light availability and positive feedback switches that modify soils to its advantage (e.g., acidity, allelopathic compounds). However, beech bark disease, a scale insect-fungus complex, is already widespread, especially in beech-dominate forests, and will likely more easily endure due to milder

winters and decreased snow cover under climate change, thus potentially leading to a major decline in American beech in future decades (Cale et al. 2017; Stephanson and Ribarik Coe, 2017). Under RCP8.5, regional models for the study region predict that the current average temperature will increase from 2-3 °C to 6 °C over the 2041-2070 horizon relative to the 1981-2010 reference period (fifth-generation Canadian Regional Climate Model, CRCM5, Martynov et al., 2013; Šeparović et al., 2013). On the one hand, the study site is at the very northern limit of the distribution of American beech and as such, it could become more favorable to beech and other southern tree species under climate change. The ability of hardwood-beech stands to regulate their soil water potential could also specifically favor beech recruitment (re: positive feedback switch). On the other hand, if beech bark disease stimulated by droughts also leads to a dieback at these latitudes, this could offer a short window of opportunities for the recruitment of other tree species that perform better in cooler soils with more available moisture while tolerating the forest floor conditions left by beech litter (e.g., greater acidity and allelopathic compounds, thick leaf litter mat).

Conclusion

The field of data science, which goes beyond static statistical approaches, allows for a thorough analysis of time series and thus provides new opportunities to study the complexity of tree-soil water dynamics and to elucidate interactions occurring at different timescales (Konings et al., 2021). In this study at a forest site in southern Quebec, Canada, mixedwoods, composed mostly of fir and maple, are exhibiting more signs of vulnerability in regard to water deficit in the context of a changing climate. Stands composed of fir and maple trees seem to have a lesser capacity to conserve soil water during a drought and to return to normal soil water states after a dry down compared to stands composed of maple and beech, which have developed regulation strategies that do both well. Because the third forest type studied, i.e., stands composed of maple and birch, have a behavior falling between the two other stands, it is believed that the soil water regulation strategies are largely attributed to beech, whereas the poor adaptation to drought is attributed to fir and other companion conifers (e.g., hemlock). Notably, forests with beech trees appear to bring (hydraulic) diversity that enhances the regulation of their soil temperature and water potential and can prove beneficial during droughts (Anderegg et al., 2018; Grossiord, 2020b). This could partly contribute to explaining the expansion of beech trees in northeastern North America, among many other causes, as observed since the 1970s. In Europe, Norway spruce benefits from the presence of European beech under drought conditions (Motte et al., 2023) as the latter allows the former to set up a faster process of acclimation (Pretzsch et al., 2020), but at the expense of beech (Thurm et al., 2016). Similarly in North America, beech could have a role to play as a companion species to maple, fir, and other plant species under climate change because of its greater capacity to maintain and restore soil water availability. This means that beech could favor soil hydroclimatic conditions that are conducive to its own maintenance and the maintenance of local plant species under climate change as well as to the migration of other plant species that are not adapting well to warmer and drier conditions in the south.

Declaration of Competing Interest

The authors declare that they have no known competing financial interests or personal relationships that could have influenced the work reported in this paper.

Acknowledgments

as well as the staff at *Station de Biologie des Laurentides* for providing access to the site and research facilities.

References

Allen, C. D., Macalady, A. K., Chenchouni, H., Bachelet, D., McDowell, N., Vennetier, M., Kitzberger, T., Rigling, A., Breshears, D. D., Hogg, E. H. (Ted), Gonzalez, P., Fensham, R., Zhang, Z., Castro, J., Demidova, N., Lim, J. H., Allard, G., Running, S. W., Semerci, A., & Cobb, N. (2010). A global overview of drought and heat-induced tree mortality reveals emerging climate change risks for forests. *Forest Ecology and Management*, *259*(4), 660–684. https://doi.org/10.1016/j.foreco.2009.09.001

Allen, C. D., Breshears, D. D., & McDowell, N. G. (2015). On underestimation of global vulnerability to tree mortality and forest die-off from hotter drought in the Anthropocene. *Ecosphere*, *6*(8), 1–55. https://doi.org/10.1890/ES15-00203.1

Anderegg, W. R. L., Konings, A. G., Trugman, A. T., Yu, K., Bowling, D. R., Gabbitas, R., Karp, D. S., Pacala, S., Sperry, J. S., Sulman, B. N., & Zenes, N. (2018). Hydraulic diversity of forests regulates ecosystem resilience during drought. *Nature*, *561*(7724), 538–541. https://doi.org/10.1038/s41586-018-0539-7

Anderegg, W.R.L., Schwalm, C., Biondi, F., Camarero, J. J., Koch, G., Litvak, M., Ogle, K., Shaw, J. D., Shevliakova, E., Williams, A. P., Wolf, A., Ziaco, E., & Pacala, S. (2015). Pervasive drought legacies in forest ecosystems and their implications for carbon cycle models. *Science*, *349*(6247), 528–532. https://doi.org/10.1126/science.aab1833

Begueria, S., Vicente-Serrano, S.M., Reig, F., Latorre, B. 2014. Standardized precipitation evapotranspiration index (SPEI) revisited: parameter fitting, evapotranspiration models, tools, datasets and drought monitoring. *International Journal of Climatology, 34*, 3001-3023. https://doi.org/10.1002/joc.3887

Bélanger, N., Holmden, C., Courchesne, F., Côté, B., & Hendershot, W. H. (2012). Constraining soil mineral weathering 87Sr/ 86Sr for calcium apportionment studies of a deciduous forest growing on soils developed from granitoid igneous rocks. *Geoderma*, *185–186*, 84–96. https://doi.org/10.1016/j.geoderma.2012.03.024

Bélanger, N., Collin, A., Khlifa, R., & Lebel-Desrosiers, S. (2021). Balsam Fir and American Beech Influence Soil Respiration Rates in Opposite Directions in a Sugar Maple Forest Near Its Northern Range Limit. *Frontiers in Forests and Global Change*, *4*. https://doi.org/10.3389/ffgc.2021.664584

Berg, A., & Sheffield, J. (2018). Soil Moisture-Evapotranspiration Coupling in CMIP5 Models: Relationship with Simulated Climate and Projections. *Journal of Climate*, *31*. https://doi.org/10.1175/JCLI-D-17

Bonsal, B.R., Aider, R., Gachon, P., Lapp, S. (2013). An assessment of Canadian prairie drought: past, present, and future. *Climate Dynamics*, *41*, 501-516. https://doi.org/10.1007/s00382-012-1422-0

Box, G., Jenkins, G. et Reinsel, G. (2008). Time Series Analysis: Forecasting and Control. 4rd ed. NJ : Prentice Hall.

Breiman, L, Friedman, J., Olshen, R. et Stone, C. (1984). Classification and Regression Trees. FL : Chapman & Hall.

Breshears, D. D., Cobb, N. S., Rich, P. M., Price, K. P., Allen, C. D., Balice, R. G., Romme, W. H., Kastens, J. H., Floyd, M. L., Belnap, J., Anderson, J. J., Myers, O. B., Meyer, C. W., & Mooney, H. A. (2005). *Regional vegetation die-off in response to global-change-type drought*. www.wrcc.dri.edu;

Brzostek, E. R., Dragoni, D., Schmid, H. P., Rahman, A. F., Sims, D., Wayson, C. A., Johnson, D. J., & Phillips, R. P. (2014). Chronic water stress reduces tree growth and the carbon sink of deciduous hardwood forests. *Global Change Biology*, *20*(8), 2531–2539. https://doi.org/10.1111/gcb.12528

Cale, J. A., Garrison-Johnston, M. T., Teale, S. A., & Castello, J. D. (2017). Beech bark disease in North America: Over a century of research revisited. In *Forest Ecology and Management* (Vol. 394, pp. 86–103). Elsevier B.V. https://doi.org/10.1016/j.foreco.2017.03.031

Canarini, A., Schmidt, H., Fuchslueger, L., Martin, V., Herbold, C. W., Zezula, D., Gündler, P., Hasibeder, R., Jecmenica, M., Bahn, M., & Richter, A. (2021). Ecological memory of recurrent drought modifies soil processes via changes in soil microbial community. *Nature Communications*, *12*(1). https://doi.org/10.1038/s41467-021-25675-4

Chen, Z., Li, S., Wan, X., Liu, S. (2022). Strategies of tree species to adapt to drought from leaf stomatal regulation and stem embolism resistance to root properties. *Front. Plant Sci. 13*:926535. doi: 10.3389/fpls.2022.926535

Cholet, C., Houle, D., Sylvain, J. D., Doyon, F., & Maheu, A. (2022). Climate Change Increases the Severity and Duration of Soil Water Stress in the Temperate Forest of Eastern North America. *Frontiers in Forests and Global Change*, *5*. https://doi.org/10.3389/ffgc.2022.879382

Collin, A., Messier, C., Kembel, S. W., & Bélanger, N. (2017a). Low light availability associated with American beech is the main factor for reduced sugar maple seedling survival and growth rates in a hardwood forest of Southern Quebec. *Forests*, *8*(11). https://doi.org/10.3390/f8110413

Collin, A., Messier, C., & Bélanger, N. (2017b). Conifer Presence May Negatively Affect Sugar Maple's Ability to Migrate into the Boreal Forest Through Reduced Foliar Nutritional Status. *Ecosystems*, *20*(4), 701–716. https://doi.org/10.1007/s10021-016-0045-4

Daszkowska-Golec, A., & Szarejko, I. (2013). Open or close the gate - Stomata action under the control of phytohormones in drought stress conditions. *Frontiers in Plant Science*, *4*. https://doi.org/10.3389/fpls.2013.00138

DeSoto, L., Cailleret, M., Sterck, F., Jansen, S., Kramer, K., Robert, E. M. R., Aakala, T., Amoroso, M. M., Bigler, C., Camarero, J. J., Čufar, K., Gea-Izquierdo, G., Gillner, S., Haavik, L. J., Hereş, A. M., Kane, J. M., Kharuk, V. I., Kitzberger, T., Klein, T., … Martínez-Vilalta, J. (2020). Low growth resilience to drought is related to future mortality risk in trees. *Nature Communications*, *11*(1). https://doi.org/10.1038/s41467-020-14300-5

D'Orangeville, L., Maxwell, J. T., Kneeshaw, D. D., Pederson, N., Duchesne, L., Logan, T., Houle, D., Arseneault, D., Beier, C. M., Bishop, D. A., Druckenbrod, D. L., Fraver, S., Girard, F., Halman, J. M., Hansen, C., Hart, J. L., Hartmann, H., Kaye, M., LeBlanc, D. C., Phillips, R. P. (2018). Drought timing and local climate determine the sensitivity of eastern temperate forests to drought. *Global Change Biology*, *24*, 2339–2351. https://doi.org/10.1111/gcb.14096

Forzieri, G., Dakos, V., McDowell, N. G., Ramdane, A., & Cescatti, A. (2022). Emerging signals of declining forest resilience under climate change. *Nature*, *608*(7923), 534–539. https://doi.org/10.1038/s41586-022-04959-9

Fu, Z., Ciais, P., Makowski, D., Bastos, A., Stoy, P. C., Ibrom, A., Knohl, A., Migliavacca, M., Cuntz, M., Šigut, L., Peichl, M., Loustau, D., El-Madany, T. S., Buchmann, N., Gharun, M., Janssens, I., Markwitz, C., Grünwald, T., Rebmann, C., … Wigneron, J. P. (2022). Uncovering the critical soil moisture thresholds of plant water stress for European

ecosystems. *Global Change Biology*, *28*(6), 2111–2123.
https://doi.org/10.1111/gcb.16050

Geßler, A., Keitel, C., Kreuzwieser, J., Matyssek, R., Seiler, W., Rennenberg, H. (2007)
Potential risks for European beech (Fagus sylvatica L.) in a changing climate. *Trees, 21*, 1–
11. https://doi.org/10.1007/s00468-006-0107-x

Grant, G. E., Tague, C. L., & Allen, C. D. (2013). Watering the forest for the trees: An
emerging priority for managing water in forest landscapes. *Frontiers in Ecology and the
Environment*, *11*(6), 314–321. https://doi.org/10.1890/120209

Greenwood, S., Ruiz-Benito, P., Martínez-Vilalta, J., Lloret, F., Kitzberger, T., Allen, C. D.,
Fensham, R., Laughlin, D. C., Kattge, J., Bönisch, G., Kraft, N. J. B., & Jump, A. S. (2017).
Tree mortality across biomes is promoted by drought intensity, lower wood density and
higher specific leaf area. *Ecology Letters*, *20*(4), 539–553.
https://doi.org/https://doi.org/10.1111/ele.12748

Grossiord, C., Buckley, T. N., Cernusak, L. A., Novick, K. A., Poulter, B., Siegwolf, R. T. W.,
Sperry, J. S., & McDowell, N. G. (2020a). Plant responses to rising vapor pressure deficit.
In *New Phytologist* (Vol. 226, Issue 6, pp. 1550–1566). Blackwell Publishing Ltd.
https://doi.org/10.1111/nph.16485

Grossiord, C. (2020b). Having the right neighbors: how tree species diversity modulates
drought impacts on forests. In *New Phytologist* (Vol. 228, Issue 1, pp. 42–49). Blackwell
Publishing Ltd. https://doi.org/10.1111/nph.15667

Hammond, W. M., Williams, A. P., Abatzoglou, J. T., Adams, H. D., Klein, T., López, R., Sáenz-
Romero, C., Hartmann, H., Breshears, D. D., & Allen, C. D. (2022). Global field
observations of tree die-off reveal hotter-drought fingerprint for Earth's forests. *Nature
Communications*, *13*(1), 1761. https://doi.org/10.1038/s41467-022-29289-2

Hammond, W.M. (2020). A matter of life and death: alternative stable states in trees, from
xylem to ecosystems. *Frontiers in Forests and Global Change, 3*:560409.
https://doi.org/10.3389/ffgc.2020.560409

Hammond, W. M., Yu, K., Wilson, L. A., Will, R. E., Anderegg, W. R. L., & Adams, H. D. (2019).
Dead or dying? Quantifying the point of no return from hydraulic failure in drought-
induced tree mortality. *New Phytologist*, *223*(4), 1834–1843.
https://doi.org/10.1111/nph.15922

Hesse, B., Gebhardt, T., Hafner, B., Hikino, K., Reitsam, A., Gigl, M., Dawid, C., Häberle, K-H.,
Grams, T. (2023). Physiological recovery of tree water relations upon drought release—
response of mature beech and spruce after five years of recurrent summer drought, *Tree
Physiology*, *43* (4), 522-538. https://doi.org/10.1093/treephys/tpac135

Hogg, E. H., Brandt, J. P., & Kochtubajda, B. (2002). Growth and dieback of aspen forests in
northwestern Alberta, Canada, in relation to climate and insects. *Canadian Journal of
Forest Research*, *32*(5), 823–832. https://doi.org/10.1139/x01-152

Holling, C. (1996). Engineering resilience versus ecological resilience. Dans P. Schulze (dir.).
Engineering within Ecological Constraints, 31–43., Washington DC. National Academy
Press.

Houle, D., Bouffard, A., Duchesne, L., Logan, T., & Harvey, R. (2012). Projections of future soil
temperature and water content for three Southern Quebec forested sites. *Journal of
Climate*, *25*(21), 7690–7701. https://doi.org/10.1175/JCLI-D-11-00440.1

Irmak, S., Payero, J., VanDeWalle, B., Rees, J., Zoubek, G., Martin, D., Kranz, W., Eisenhauer,
D. et Leininger, D. (2016). Principles and operational characteristics of watermark
granular matrix sensor to measure soil water status and its practical applications for

irrigation management in various soil textures. EC783, University of Nebraska-Lincoln Extension.

Jacques, C., Salon, C., Barnard, R. L., Vernoud, V., & Prudent, M. (2021). Drought stress memory at the plant cycle level: A review. *Plants*, *10*(9). https://doi.org/10.3390/plants10091873

Johnstone, J. F., Allen, C. D., Franklin, J. F., Frelich, L. E., Harvey, B. J., Higuera, P. E., Mack, M. C., Meentemeyer, R. K., Metz, M. R., Perry, G. L. W., Schoennagel, T., & Turner, M. G. (2016). Changing disturbance regimes, ecological memory, and forest resilience. *Frontiers in Ecology and the Environment*, *14*(7), 369–378. https://doi.org/10.1002/fee.1311

Kannenberg, S. A., Schwalm, C. R., & Anderegg, W. R. L. (2020). Ghosts of the past: how drought legacy effects shape forest functioning and carbon cycling. In *Ecology Letters*, *23*(5), 891–901. https://doi.org/10.1111/ele.13485

Kögler, F., & Söffker, D. (2020). State-based open-loop control of plant growth by means of water stress training. *Agricultural Water Management*, *230*. https://doi.org/10.1016/j.agwat.2019.105963

Konings, A. G., Saatchi, S. S., Frankenberg, C., Keller, M., Leshyk, V., Anderegg, W. R. L., Humphrey, V., Matheny, A. M., Trugman, A., Sack, L., Agee, E., Barnes, M. L., Binks, O., Cawse-Nicholson, K., Christoffersen, B. O., Entekhabi, D., Gentine, P., Holtzman, N. M., Katul, G. G., … Zuidema, P. A. (2021). Detecting forest response to droughts with global observations of vegetation water content. *Global Change Biology*, *27*(23), 6005–6024. https://doi.org/10.1111/gcb.15872

Koster, R. D., & Suarez, M. J. (2001). Soil Moisture Memory in Climate Models. *Journal of Hydrometeorology*, *2,* 558-570. https://doi.org/10.1175/1525-7541(2001)002<0558:SMMICM>2.0.CO;2

Lajeunesse, D. (1990). Le système racinaire de quelques érablières du Québec. MSc thesis, Department of Renewable Resources, McGill University, Montreal.

Leuschner, C. (2020). Drought response of European beech (Fagus sylvatica L.) — A review. *Perspectives in Plant Ecology, Evolution and Systematics, 47: 125576* https://doi.org/10.1016/j.ppees.2020.125576

Lloret, F., Jaime, L. A., Margalef-Marrase, J., Pérez-Navarro, M. A., & Batllori, E. (2022). Short-term forest resilience after drought-induced die-off in Southwestern European forests. *Science of the Total Environment*, *806*. https://doi.org/10.1016/j.scitotenv.2021.150940

The MathWorks Inc. (2022). MATLAB version: 9.12.0 (R2022a), Natick, Massachusetts: The MathWorks Inc. https://www.mathworks.com

Martínez-Vilalta, J., Poyatos, R., Aguadé, D., Retana, J., & Mencuccini, M. (2014). A new look at water transport regulation in plants. *New Phytologist*, *204*(1), 105–115. https://doi.org/10.1111/nph.12912

Martínez-Vilalta J, Garcia-Forner N. (2017). Water potential regulation, stomatal behaviour and hydraulic transport under drought: deconstructing the iso/anisohydric concept. *Plant, Cell & Environment, 40*, 962–976. https://doi.org/10.1111/pce.12846

Martynov, A., Laprise, R., Sushama, L., Winger, K., Šeparovic`, L., & Dugas, B. (2013). Reanalysis-driven climate simulation over CORDEX North America domain using the Canadian Regional Climate Model, version 5: Model performance evaluation. *Climate Dynamics*, *41*, 2973–3005. https://doi.org/10.1007/s00382-013-1778-9

McColl, K. A., Wang, W., Peng, B., Akbar, R., Short Gianotti, D. J., Lu, H., Pan, M., & Entekhabi, D. (2017). Global characterization of surface soil moisture drydowns. *Geophysical Research Letters*, *44*(8), 3682–3690. https://doi.org/10.1002/2017GL072819

McDowell, N. G., & Allen, C. D. (2015). Darcy's law predicts widespread forest mortality under climate warming. *Nature Climate Change*, *5*(7), 669–672. https://doi.org/10.1038/nclimate2641

McDowell, N., Pockman, W. T., Allen, C. D., Breshears, D. D., Cobb, N., Kolb, T., Plaut, J., Sperry, J., West, A., Williams, D. G., & Yepez, E. A. (2008). Mechanisms of plant survival and mortality during drought: Why do some plants survive while others succumb to drought? *New Phytologist*, *178*(4), 719–739. https://doi.org/10.1111/j.1469-8137.2008.02436.x

Meinzer, F.C., Woodruff, D.R., Marias, D.E., Smith, D.D., McCulloh, K.A., Howard, A.R. and Magedman, A.L. (2016). Mapping 'hydroscapes' along the iso- to anisohydric continuum of stomatal regulation of plant water status. *Ecol Lett, 19*: 1343-1352. https://doi.org/10.1111/ele.12670

Michaelina, M., Hogg, E.H., Hall, R.J., Arsenault, E. (2011). Massive mortality of aspen following severe drought along the southern edge of the Canadian boreal forest. *Global Change Biology*, *17*, 2084-2094. https://doi.org/10.1111/j.1365-2486.2010.02357.x

Monteith, J. et Unsworth, M. (2007). Principles of Environmental Physics (3 éd.). Elsevier Science.

Motte, F., Rötzer, T., Biber, P., Uhl, E., Pritsch, K., Pretzsch, H. (2023). Growth of European beech recovered faster than that of Norway spruce after a five-year experimental drought in a mixed forest stand. *Trees, 37*, 1695–1715. https://doi.org/10.1007/s00468-023-02453-x

Müller, L. M., & Bahn, M. (2022). Drought legacies and ecosystem responses to subsequent drought. *Global Change Biology*, *28*(17), 5086–5103. https://doi.org/10.1111/gcb.16270

Nelson, S. K., & Oliver, M. J. (2017). A Soil-Plate Based Pipeline for Assessing Cereal Root Growth in Response to Polyethylene Glycol (PEG)-Induced Water Deficit Stress. *Frontiers in plant science*, *8*, 1272. https://doi.org/10.3389/fpls.2017.01272

Nikolova, P. S., Bauerle, T. L., Häberle, K. H., Blaschke, H., Brunner, I., & Matyssek, R. (2020). Fine-Root Traits Reveal Contrasting Ecological Strategies in European Beech and Norway Spruce During Extreme Drought. *Frontiers in Plant Science*, *11*. https://doi.org/10.3389/fpls.2020.01211

Nolet, P., & Kneeshaw, D. (2018). Extreme events and subtle ecological effects: lessons from a long-term sugar maple–American beech comparison. *Ecosphere*, *9*(7). https://doi.org/10.1002/ecs2.2336

Ogle, K., Barber, J. J., Barron-Gafford, G. A., Bentley, L. P., Young, J. M., Huxman, T. E., Loik, M. E., & Tissue, D. T. (2015). Quantifying ecological memory in plant and ecosystem processes. *Ecology Letters*, *18*(3), 221–235. https://doi.org/https://doi.org/10.1111/ele.12399

Orth, R., & Seneviratne, S. I. (2012). Analysis of soil moisture memory from observations in Europe. *Journal of Geophysical Research Atmospheres*, *117*(15). https://doi.org/10.1029/2011JD017366

Payero, J. O., Qiao, X., Khalilian, A., Mirzakhani-Nafchi, A., & Davis, R. (2017). Evaluating the Effect of Soil Texture on the Response of Three Types of Sensors Used to Monitor Soil Water Status. *Journal of Water Resource and Protection*, *09*(06), 566–577. https://doi.org/10.4236/jwarp.2017.96037

Peltier, D. M. P., Guo, J., Nguyen, P., Bangs, M., Wilson, M., Samuels-Crow, K., Yocom, L. L., Liu, Y., Fell, M. K., Shaw, J. D., Auty, D., Schwalm, C., Anderegg, W. R. L., Koch, G. W., Litvak, M. E., & Ogle, K. (2022). Temperature memory and non-structural carbohydrates

mediate legacies of a hot drought in trees across the southwestern USA. *Tree Physiology*, *42*(1), 71–85. https://doi.org/10.1093/treephys/tpab091

Pendergrass, A. G., Meehl, G. A., Pulwarty, R., Hobbins, M., Hoell, A., AghaKouchak, A., Bonfils, C. J. W., Gallant, A. J. E., Hoerling, M., Hoffmann, D., Kaatz, L., Lehner, F., Llewellyn, D., Mote, P., Neale, R. B., Overpeck, J. T., Sheffield, A., Stahl, K., Svoboda, M., … Woodhouse, C. A. (2020). Flash droughts present a new challenge for subseasonal-to-seasonal prediction. *Nature Climate Change*, *10*(3), 191–199. https://doi.org/10.1038/s41558-020-0709-0

Peng, C., Ma, Z., Lei, X., Zhu, Q., Chen, H., Wang, W., Liu, S., Li, W., Fang, X., & Zhou, X. (2011). A drought-induced pervasive increase in tree mortality across Canada's boreal forests. *Nature Climate Change*, *1*(9), 467–471. https://doi.org/10.1038/nclimate1293

Pretzsch, H., Grams, T., Häberle, K. H., Pritsch, K., Bauerle, T., & Rötzer, T. (2020). Growth and mortality of Norway spruce and European beech in monospecific and mixed-species stands under natural episodic and experimentally extended drought. Results of the KROOF throughfall exclusion experiment. *Trees*, *34*(4), 957–970. https://doi.org/10.1007/s00468-020-01973-0

Puchi, P. F., Dalmonech, D., Vangi, E., Battipaglia, G., Tognetti, R., & Collalti, A. (2024). Contrasting patterns of water use efficiency and annual radial growth among European beech forests along the Italian peninsula. Scientific reports, 14(1), 6526. https://doi.org/10.1038/s41598-024-57293-7

Ratzmann, G., Meinzer, F. C., & Tietjen, B. (2019). Iso/Anisohydry: Still a Useful Concept. *Trends in Plant Science*, *24*(3), 191–194. https://doi.org/https://doi.org/10.1016/j.tplants.2019.01.001

Régnière, J., Bolstad, P. (1994). Statistical simulation of daily air temperature patterns eastern North America to forecast seasonal events in insect pest management, *Environmental Entomology*, *23*(6), 1368–1380. https://doi.org/10.1093/ee/23.6.1368

Régnière, J., Saint-Amand, R. (2017). BioSIM 11. Rapport d'information LAU-X-129, Ressources naturelles Canada, Service canadien des forêts, Centre de foresterie des Laurentides.

Rukh, S., Sanders, T.G.M., Krüger, I., Schad, T., Bolte, A. (2023). Distinct Responses of European Beech (Fagus sylvatica L.) to Drought Intensity and Length—A Review of the Impacts of the 2003 and 2018–2019 Drought Events in Central Europe. *Forests, 14*(2), 248. https://doi.org/10.3390/f14020248

Samaniego, L., Thober, S., Kumar, R., Wanders, N., Rakovec, O., Pan, M., et al. (2018). Anthropogenic warming exacerbates European soil moisture droughts. *Nat. Clim. Change* 8, 421–426. https://doi.org/10.1038/s41558-018-0138-5

Sánchez-Pinillos, M., D'Orangeville, L., Boulanger, Y., Comeau, P., Wang, J., Taylor, A. R., & Kneeshaw, D. (2022). Sequential droughts: A silent trigger of boreal forest mortality. *Global Change Biology*, *28*(2), 542–556. https://doi.org/10.1111/gcb.15913

Saucier, J.-P., Robitaille, A., and Grondin, P. (2009). "Cadre bioclimatique du Québec," in Manuel de Foresterie, 2ième édition, ed. Ordre des ingénieurs forestiers du Québec (Québec, QC: MultiMondes), 186–205.

Savitzky, A. et Golay, M. J. E. (1964). Smoothing and differentiation of data by simplified least squares procedures. *Analytical Chemistry, 36*, 1627–1639. http://dx.doi.org/10.1021/ac60214a047

Seneviratne, S. I., Corti, T., Davin, E. L., Hirschi, M., Jaeger, E. B., Lehner, I., Orlowsky, B., & Teuling, A. J. (2010). Investigating soil moisture–climate interactions in a changing

climate: A review. *Earth-Science Reviews*, *99*(3), 125–161. https://doi.org/https://doi.org/10.1016/j.earscirev.2010.02.004

Senf, C., Buras, A., Zang, C. S., Rammig, A., & Seidl, R. (2020). Excess forest mortality is consistently linked to drought across Europe. *Nature Communications*, *11*(1). https://doi.org/10.1038/s41467-020-19924-1

Šeparović, L., Alexandru, A., Laprise, R., Martynov, A., Sushama, L., Winger, K., Valin, M. (2013). Present climate and climate change over North America as simulated by the fifth-generation Canadian Regional Climate Model. *Climate Dynamics*, *41*(11–12), 3167–3201. https://doi.org/10.1007/s00382-013-1737-5

Shock, C., Barnum, J. and Seddigh, M. (1998). Calibration of watermark soil moisture sensors for irrigation management. Available at : https://www.researchgate.net/publication/228762944_Calibration_of_W_ermark_Soil_Moisture_Sensors_for_Irrigation_Management (Accessed: 14 March 2024)

Shock, C. C., & Wang, F.-X. (2011). Soil Water Tension, a Powerful Tool for Productivity and Stewardship. *HortScience*, *46*(2), 178–185. https://doi.org/10.21273/HORTSCI.46.2.178

Slette, I. J., Post, A. K., Awad, M., Even, T., Punzalan, A., Williams, S., Smith, M. D., & Knapp, A. K. (2019). How ecologists define drought, and why we should do better. *Global Change Biology*, *25*(10), 3193–3200. https://doi.org/10.1111/gcb.14747

Soil Classification Working Group. (1998). The Canadian System of Soil Classification (3 ed.). Ottawa : Agriculture and Agri-Food Canada Publication and NRC Research Press. Available at: https://sis.agr.gc.ca/cansis/publications/manuals/1998-cssc-ed3/index.html

Stephanson, C. A., & Coe, N. R. (2017). Impacts of beech bark disease and climate change on American beech. In *Forests* (Vol. 8, Issue 5). MDPI AG. https://doi.org/10.3390/f8050155

Stevenson, S., Coats, S., Touma, D., Cole, J., Lehner, F., Fasullo, J., & Otto-Bliesner, B. (2022). Twenty-first century hydroclimate: A continually changing baseline, with more frequent extremes. *Proceedings of the National Academy of Sciences*, *119*(12), 1–9. https://doi.org/10.1073/pnas.2108124119

St-Jean, É., Meunier, S., Nolet, P., Messier, C., & Achim, A. (2021). Increased levels of harvest may favour sugar maple regeneration over American beech in northern hardwoods. *Forest Ecology and Management*, *499*. https://doi.org/10.1016/j.foreco.2021.119607

Tetens, O. (1930). Über einige meteorologische Begriffe. Zeitschrift für geophysik. Friedrich Vieweg & Sohn Akt.- Gesellschaft.

Thurm, E. A., Uhl, E., & Pretzsch, H. (2016). Mixture reduces climate sensitivity of Douglas-fir stem growth. *Forest Ecology and Management*, *376*, 205–220. https://doi.org/https://doi.org/10.1016/j.foreco.2016.06.020

Trenberth, K. E., Dai, A., Van Der Schrier, G., Jones, P. D., Barichivich, J., Briffa, K. R., & Sheffield, J. (2014). Global warming and changes in drought. *Nature Climate Change,* *4*(1), 17–22. https://doi.org/10.1038/nclimate2067

Trumbore, S., Brando, P., & Hartmann, H. (2015). Forest health and global change. *Science,* *349*(6250), 814–818. American Association for the Advancement of Science. https://doi.org/10.1126/science.aac6759

Walthert, L., Ganthaler, A., Mayr, S., Saurer, M., Waldner, P., Walser, M., Zweifel, R., & von Arx, G. (2021). From the comfort zone to crown dieback: Sequence of physiological stress thresholds in mature European beech trees across progressive drought. The Science of the total environment, 753, 141792. https://doi.org/10.1016/j.scitotenv.2020.141792

Williams, A. P., Cook, E. R., Smerdon, J. E., Cook, B. I., Abatzoglou, J. T., Bolles, K., Baek, S. H., Badger, A. M., and Livneh, B. (2020). Large contribution from anthropogenic warming to

an emerging North American megadrought. *Science, 368*, 314–318.
https://doi.org/10.1126/science.aaz9600

Yao, Y., Fu, B., Liu, Y., Li, Y., Wang, S., Zhan, T., Wang, Y., & Gao, D. (2022). Evaluation of ecosystem resilience to drought based on drought intensity and recovery time. *Agricultural and Forest Meteorology*, *314*. https://doi.org/10.1016/j.agrformet.2022.108809

Zhao, Z., Zhang, Y., Liu, L., & Hu, Z. (2018). The impact of drought on vegetation conditions within the Damqu River Basin, Yangtze River Source Region, China. *PLoS ONE*, *13*(8). https://doi.org/10.1371/journal.pone.0202966

Supplementary materials
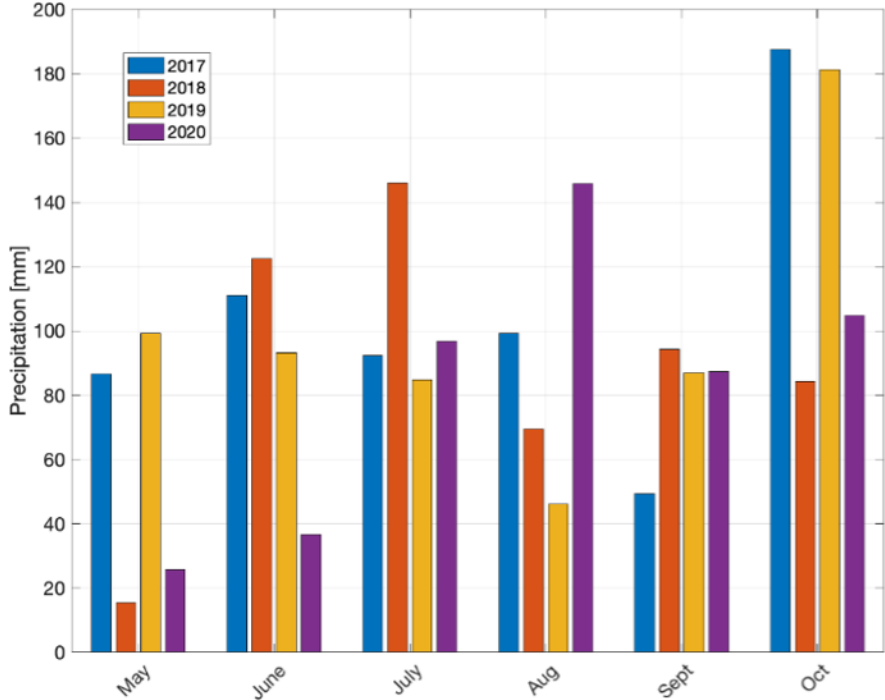
Figure S1: Growing season precipitation (May to October) in mm at the *Station de Biologie des Laurentides* between 2017 and 2020. Data are from the BioSIM model.
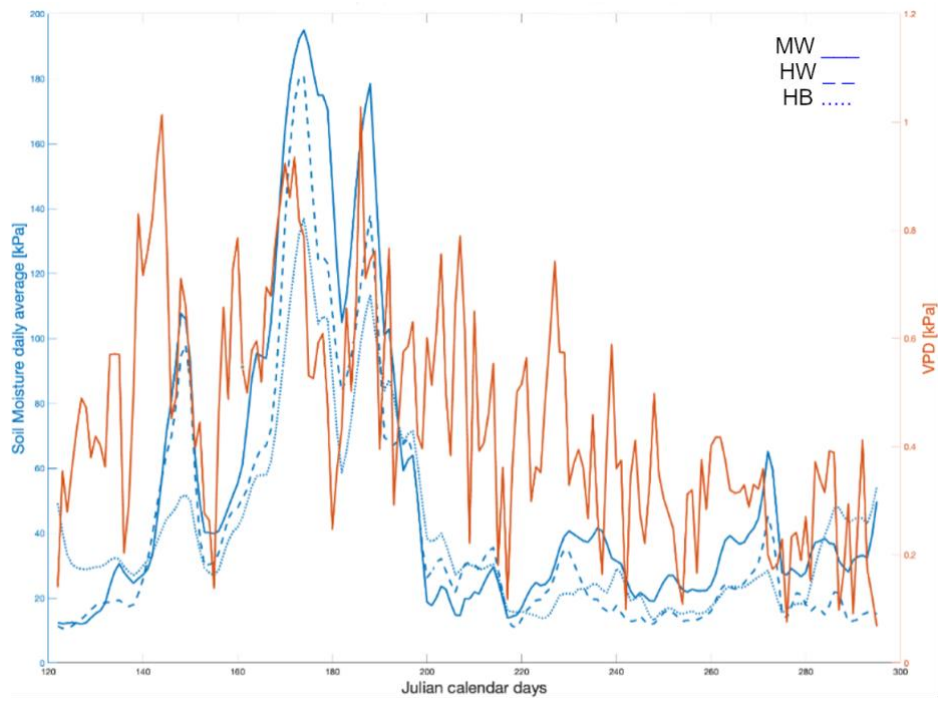
Figure S2: Dynamics of soil water potential in kPa (blue) and vapor pressure deficit in kPa (orange) from May to October 2020 (expressed as Julian calendar days) for mixedwoods (MW), hardwoods (HW) and hardwood-beech stands (HB). Data are daily averages.
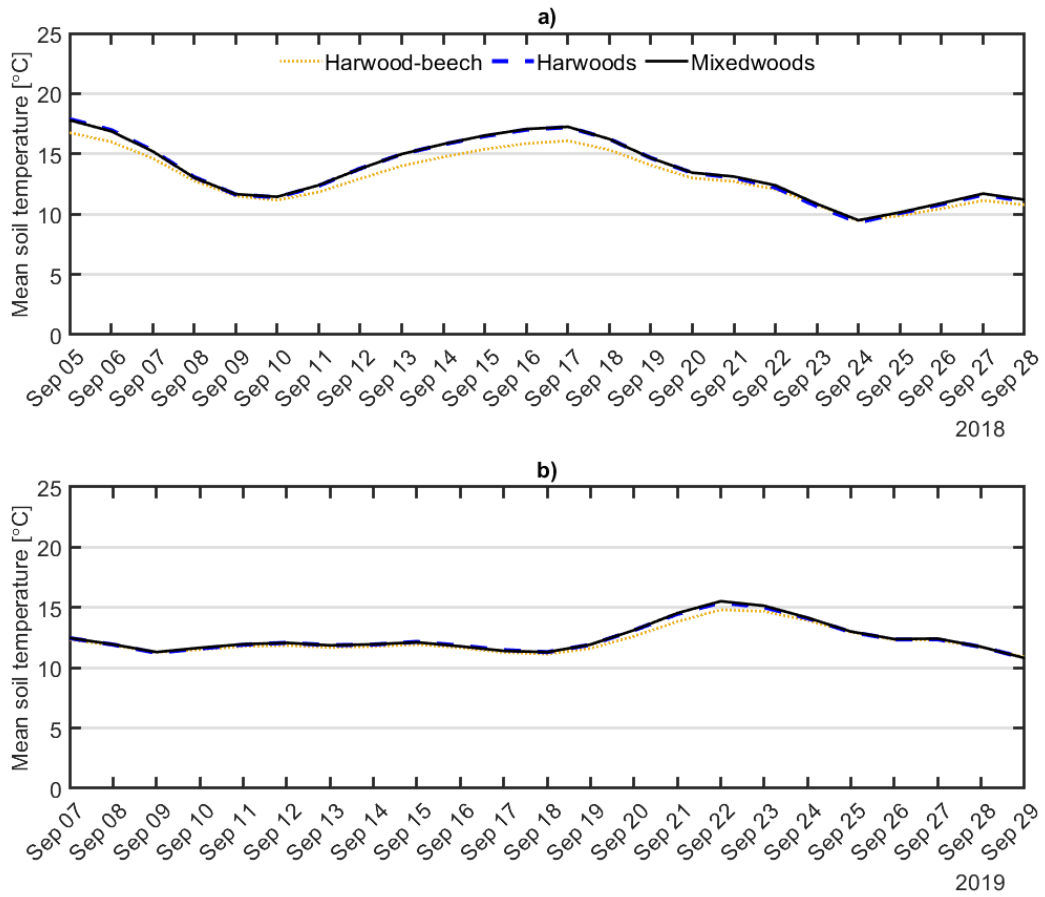
Figure S3: Dynamics of soil temperature in °C during a flash drought period in (a) September 2018 and (b) September 2019 for mixedwoods, hardwoods and hardwood-beech stands. Dry-down in 2018 is from September 13th to September 20th, and from September 15th to September 21st in 2019.

Table S1: Pearson correlations between meteorological variables (p < 0.05).

	Prcp	RelH	SRad	Tair	VPD
Prcp					
RelH	0,42				
SRad	-0,50	-0,80			
Tair	0,05	0,07	0,18		
VPD	-0,38	-0,81	0,77	0,46	

Table S2: Pearson correlations between soil water potential (SWP) and meteorological variables and soil temperature for mixedwoods (MW), hardwoods (HW) and hardwood-beech stands (HB) individually (p < 0.05).

	Prcp	RelH	SRad	Tair	VPD	Tsoil
SWP_{MW}	-0,04	-0,28	0,32	0,53	0,57	0,42
SWP_{HW}	-0,02	-0,23	0,25	0,45	0,49	0,33
SWP_{HB}	0,00	-0,27	0,25	0,39	0,49	0,25

Prcp is precipitation, RelH is relative humidity, SRad is solar radiation, Tair is air temperature, VPD is vapor pressure deficit and Tsoil is soil temperature.

Table S3: Cross-correlation coefficients obtained for mixedwoods in 2020. Red indicates high values, blue indicates value at lag-0 and bold values are the highest value for each variable/column.

	Tsoil	VPD	RelH	SRad	Prcp	Tair
t − 6 days	0.7780	0.7414	0.7176	0.6880	0.3156	0.7866
t − 5	0.7790	0.7468	**0.7182**	0.6919	0.3295	0.7884
t − 4	0.7805	0.7572	0.7169	0.7001	0.3359	0.7916
t − 3	0.7820	0.7689	0.7150	0.7106	0.3423	0.7961
t − 2	0.7831	0.7822	0.7122	0.7221	**0.3465**	0.8011
t − 1	**0.7834**	0.7981	0.7085	0.7368	0.3440	0.8050
t = 0	0.7825	0.8172	0.7042	0.7557	0.3146	**0.8078**
t + 1	0.7772	0.8313	0.6943	0.7714	0.2784	0.8051
t + 2	0.7701	**0.8380**	0.6867	0.7828	0.2534	0.7991
t + 3	0.7621	0.8372	0.6817	0.7893	0.2483	0.7901
t + 4	0.7542	0.8334	0.6784	0.7921	0.2432	0.7812
t + 5	0.7462	0.8302	0.6749	0.7959	0.2313	0.7727
t + 6	0.7376	0.8259	0.6716	**0.7986**	0.2180	0.7631

Tsoil is soil temperature, VPD is vapor pressure deficit, RelH is relative humidity, SRad is solar irradiance, Prcp is precipitation and Tair is air temperature.

Table S4: Cross-correlation coefficients obtained for hardwoods in 2020. Red indicates high values, blue indicates value at lag-0 and bold values are the highest value for each variable/column.

	Tsoil	VPD	RelH	SRad	Prcp	Tair
t − 6 days	0.7829	0.7389	**0.7108**	0.6902	0.3054	0.7928
t − 5	0.7837	0.7453	0.7095	0.6929	0.3165	0.7941
t − 4	0.7850	0.7572	0.7061	0.7001	0.3262	0.7970
t − 3	0.7868	0.7720	0.7017	0.7112	0.3359	0.8025
t − 2	0.7885	0.7881	0.6968	0.7247	**0.3416**	0.8099
t − 1	**0.7889**	0.8076	0.6899	0.7423	0.3330	0.8157
t = 0	0.7870	0.8291	0.6815	0.7630	0.2934	**0.8182**
t + 1	0.7812	0.8441	0.6709	0.7806	0.2518	0.8150
t + 2	0.7731	**0.8492**	0.6635	0.7920	0.2240	0.8076
t + 3	0.7636	0.8454	0.6590	0.7973	0.2243	0.7966
t + 4	0.7534	0.8402	0.6549	0.8005	0.2263	0.7844
t + 5	0.7430	0.8345	0.6510	0.8033	0.2218	0.7719
t + 6	0.7327	0.8264	0.6482	**0.8035**	0.2131	0.7595

Tsoil is soil temperature, VPD is vapor pressure deficit, RelH is relative humidity, SRad is solar irradiance, Prcp is precipitation and Tair is air temperature.

Table S5: Cross-correlation coefficients obtained for hardwood-beech (2020. Red indicates high values, blue indicates value at lag-0 and bold values are the highest value for each variable/column.

	Tsoil	VPD	RelH	SRad	Prcp	Tair
t – 6 days	0.8294	0.8013	0.7700	0.7503	0.3417	0.8307
t – 5	0.8304	0.8070	0.7730	0.7569	0.3546	0.8326
t – 4	0.8313	0.8154	0.7752	0.7653	0.3630	0.8340
t – 3	0.8323	0.8246	0.7771	0.7722	0.3732	0.8367
t – 2	**0.8329**	0.8342	**0.7785**	0.7824	**0.3816**	0.8416
t – 1	**0.8329**	0.8492	0.7776	0.7977	0.3808	0.8447
t = 0	0.8319	0.8657	0.7777	0.8151	0.3594	**0.8479**
t + 1	0.8247	0.8762	0.7639	0.8234	0.3274	0.8438
t + 2	0.8171	**0.8787**	0.7542	0.8282	0.3074	0.8388
t + 3	0.8090	0.8739	0.7482	0.8307	0.3017	0.8316
t + 4	0.8005	0.8661	0.7443	0.8307	0.2963	0.8228
t + 5	0.7916	0.8607	0.7393	0.8323	0.2827	0.8129
t + 6j	0.7826	0.8561	0.7337	**0.8334**	0.2647	0.8023

Tsoil is soil temperature, VPD is vapor pressure deficit, RelH is relative humidity, SRad is solar irradiance, Prcp is precipitation and Tair is air temperature.